Combinatorial Persistent Homology Transform

Brittany Terese Fasy¹ and Amit Patel²

¹School of Computing and Dept. of Mathematical Sciences, Montana State University

²Department of Mathematics, Colorado State University

Abstract

The combinatorial interpretation of the persistence diagram as a Möbius inversion was recently shown to be functorial. We employ this discovery to recast the Persistent Homology Transform of a geometric complex as a representation of a cellulation on \mathbb{S}^n to the category of combinatorial persistence diagrams. Detailed examples are provided. We hope this recasting of the PH transform will allow for the adoption of existing methods from algebraic and topological combinatorics to the study of shapes.

1 Introduction

Persistent homology (PH) captures the "shape" of a topological space often arising from data. It takes as input a filtration of a space, usually paramterized by the reals, and outputs a multiset of points in the extended plane known as the persistence diagram. Each point in the persistence diagram represents a homological "feature" of the topological space and its coordinates provide the interval of parameters for which that feature is present. Individually, a persistence diagram is a powerful data analysis tool; however, a single descriptor is often not rich enough to capture the intricacies of large, complex data. For example, the family of filtrations giving rise to the same persistence diagram can be arbitrarily large. One approach for capturing more information about a space is to consider not just one filtration of the space but a family of filtrations of the space and therefore a family of persistence diagrams.

One such family of descriptors and the focus of this paper is the *persistent homology* transform, introduced initially in [25], which takes as input a space embedded in \mathbb{R}^{N+1} and represents it—or transforms it—into a family of persistence diagrams parameterized by the set of all directions \mathbb{S}^N . The idea behind this transform goes back the early 2000s [1] and was recently generalized to weighted simplicial complexes in [17]. The PH transform is a complete representation of the original shape. That is, no two different shapes have the same

BTF is supported by the National Science Foundation under grant no. DMS 1664858. AP is supported by the Leverhulme Trust grant VP2-2021-008.

PH transform. Although \mathbb{S}^N comprises an uncountable set of directions, if K is a nicely embedded geometric simplicial complex, then it has a finite representation [2, 9, 13, 22]. The PH transform and other topological transforms have been applied using a sample of directions [3, 8, 16, 17, 20, 25], yet there is still a substantial gap between the theory and this practice [12].

Our Contributions Consider a space X with an embedding $\phi: X \to \mathbb{R}^{N+1}$. The PH transform of ϕ is the assignment to every direction $\mu \in \mathbb{S}^N$ the sublevel set persistence diagram of the height function $\phi_{\mu}: X \to \mathbb{R}$ in that direction. As mentioned above, the persistence diagram is the assignment to every interval of \mathbb{R} a natural number often called its multiplicity or, in our parlance, a charge. Unfortunately, there is a major downside to this approach. In practice, ϕ is finitely generated; for example, ϕ is a PL embedding of a finite simplicial complex. Its PH transform consists of an uncountable set of distinct persistence diagrams; however, when ignoring exact birth/death coordinates and keeping track of only the relations between birth/death coordinates, we observe that there are distinct places where combinatorial changes in the diagrams happen. We call two persistence diagrams combinatorially equivalent when the diagrams are related by a homeomorphism from \mathbb{R} to itself. In this setting, we expect that most directions $\mu \in \mathbb{S}^N$ have an open neighborhood $U \subseteq \mathbb{S}^N$ such that the persistence diagrams associated to any two directions $\nu, \nu' \in U$ are combinatorially equivalent.

In that light, we take a combinatorial approach to the PH transform by adopting the combinatorial framework of persistent homology developed by McClearly and Patel [21]. In this setting, filtrations are indexed by an abstract totally ordered, finite poset P as opposed to the real numbers. The combinatorial persistence diagram is then the assignment to every non-empty (order-theoretic) interval $[a, b] \subseteq P$ a charge. Given a PL embedding, we show that there is a cellulation of \mathbb{S}^n such that the combinatorial persistence diagrams associated to any two directions on a common cell are exactly the same. This cellular decomposition is the same decomposition observed in [2, 9, 14] for the PH transform and in [7] for vineyards. Further, we harness functoriality of McClearly and Patel to express the PH transform as a representation of the cellulation on \mathbb{S}^n to the category of combinatorial persistence diagrams and charge-preserving morphisms. The cellulation is finite and every combinatorial persistence diagram is finite making our combinatorial PH transform a finite object. We hope that this recasting of the PH transform will allow for the adoption of existing methods from algebraic and topological combinatorics to the study of shapes.

2 Preliminiaries

We use this section to establish background and notation. Section 2.1 introduces geometric complexes and their height functions. Section 2.2 introduces the combinatorial persistent homology pipeline of McClearly and Patel. See also Appendix A for a discussion of our notation on posets and categories. As mentioned in Section 1, the combinatorial persistence diagram is indexed by an abstract totally ordered, finite poset as opposed to the traditional

persistence diagram that is indexed by the real numbers. Since we are departing from traditional persistent homology and focusing solely on its combinatorial version, we drop the word "combinatorial" from our discussion of combinatorial persistent homology.

2.1 Embeddings of Simplicial Complexes

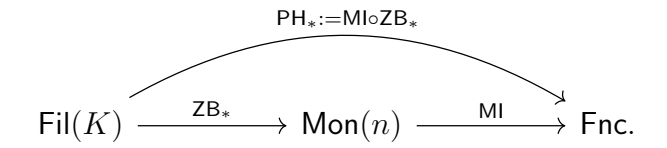
We start with an introduction to our main object of study: geometric complexes and their height functions. We adopt notation similar to [15, Section 2.1].

Fix a simplicial complex K, let $K^0 \subseteq K$ be its vertices, and denote by |K| its underlying space. For the purposes of this paper, we assume all simplicial complexes are finite. Given a function $\hat{\phi}: K^0 \to \mathbb{R}^{N+1}$ defined on its vertices, we extend it to a PL function on the entire underlying space |K| as follows. For a simplex $\sigma = [v_0, \dots, v_k]$, express every point $x \in |\sigma|$ by its barycentric coordinates (x_0, x_1, \dots, x_k) . Then, the linear extension of $\hat{\phi}$ to $|\sigma|$ is the map that sends x to the point $x_0\hat{\phi}(v_0) + x_1\hat{\phi}(v_1) + \dots + x_k\hat{\phi}(v_k)$. In this way, the function $\hat{\phi}$ extends to a PL function $\phi: |K| \to \mathbb{R}^{N+1}$ on the entire complex. If such an extension is injective, we call ϕ a geometric complex.

We are interested in examining the geometric complex $\phi: |K| \to \mathbb{R}^{N+1}$ from all directions. Denote by $\mathbb{S}^N := \{\mu \in \mathbb{R}^{N+1} : ||\mu|| = 1\}$ the sphere of all directions in \mathbb{R}^{N+1} . The *height function* on ϕ along a direction $\mu \in \mathbb{S}^N$ is the continuous function $\phi_{\mu}: |K| \to \mathbb{R}^{N+1}$ defined as the dot product $\phi_{\mu}(x) := \phi(x) \cdot \mu$. For $L \subseteq |K|$, we let $\phi_{\mu}(L) := \sup_{x \in L} \phi_{\mu}(x)$. In particular, if L is a simplex in K, then $\phi_{\mu}(L)$ is the maximum height of the vertices that define L.

2.2 Persistent Homology Pipeline

We now give a brief introduction to the persistent homology pipeline of McCleary and Patel [21] restricted to the special case of combinatorial one-parameter filtrations and to a fixed simplicial complex K. This pipeline consists of three categories Fil(K), Mon(n), and Fnc(n) and two functors ZB_* and Ml:



We call ZB_* the birth-death functor, MI the Möbius inversion functor, and the composition PH_* the persistent homology functor.

Filtrations Let ΔK be the poset consisting of subcomplexes of K ordered by inclusion. Given a finite, totally ordered poset P, a P-filtration of K is a functor $F:P\to \Delta K$ such that $F(\top)=K$. Let P and Q be finite, totally ordered posets. A filtration-preserving morphism is a triple (F,G,α) where $F:P\to \Delta K$ and $G:Q\to \Delta K$ are P- and Q-filtrations of K, respectively, and $\alpha:P\to Q$ is a bounded monotone function satisfying the following axiom. For all $a\in Q$, $G(a)=F(a^*)$, where $a^*:=\max\alpha^{-1}[\bot,a]$, i.e., the maximal element in P that maps to a:

If (F, G, α) and (G, H, β) are filtration-preserving morphisms, then the composition $(F, H, \beta \circ \alpha)$ is a filtration-preserving morphism:

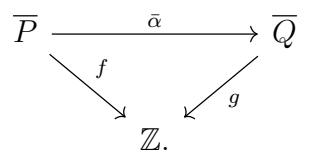
$$P \xrightarrow{\alpha} Q \xrightarrow{\beta} R$$

$$\downarrow^{G} \downarrow_{H}$$

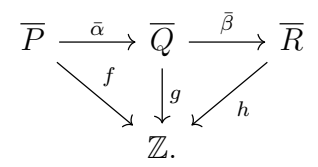
$$\Delta K.$$

Definition 2.1: Fix a simplicial complex K. Let Fil(K) be the category whose objects are P-filtrations of K, over all finite, totally ordered posets P, and whose morphisms are filtration-preserving morphisms. We call Fil(K) the **category of filtrations of** K.

Monotone Integral Functions Assume the usual total ordering on the integer \mathbb{Z} . Let P and Q be two finite, totally ordered posets and let $f: \overline{P} \to \mathbb{Z}$ and $g: \overline{Q} \to \mathbb{Z}$ be two monotone integral functions on their poset of intervals; see Appendix A. A monotone-preserving morphism is a triple $(f, g, \overline{\alpha})$, where $f: \overline{P} \to \mathbb{Z}$ and $g: \overline{Q} \to \mathbb{Z}$ are monotone integral functions and $\overline{\alpha}: \overline{P} \to \overline{Q}$ is a bounded monotone function induced by a bounded monotone function $\alpha: P \to Q$ satisfying the following axiom. For all $I \in \overline{Q}$, $g(I) = f(\max \overline{\alpha}^{-1}[\bot, I])$. In other words, for every interval I = [a, b], $g(I) = f([a^*, b^*])$ where $a^* = \max f^{-1}[\bot, a]$ and $b^* = \max f^{-1}[\bot, b]$.



If $(f, g, \bar{\alpha})$ and $(g, h, \bar{\beta})$ are two monotone-preserving morphisms, then the composition $(f, h, \bar{\beta} \circ \bar{\alpha})$ is a monotone-preserving morphism:



Definition 2.2: Let Mon be the category whose objects are monotone integral functions, over all finite, totally ordered posets, and whose morphisms are monotone-preserving morphisms. We call Mon the **category of monotone functions**.

Integral Functions Let P and Q be finite, totally ordered posets and let $\sigma: \overline{P} \to \mathbb{Z}$ and $\tau: \overline{Q} \to \mathbb{Z}$ be two *integral functions* on their poset of intervals. Let $\alpha: P \to Q$ be a bounded poset function such that for all $I \in \overline{Q}$,

$$g(I) = \sum_{J \in \alpha^{-1}(I)} f(J). \tag{1}$$

Here, if $\alpha^{-1}(I)$ is empty, then we interpret the sum as 0. We call the triple $(\sigma, \tau, \bar{\alpha})$ a charge-preserving morphism, where $\bar{\alpha} : \overline{P} \to \overline{Q}$ is the bounded poset function induced by α . If $(\sigma, \tau, \bar{\alpha})$ and $(\tau, v, \bar{\beta})$ are charge-preserving morphisms, then $(\sigma, v, \bar{\beta} \circ \bar{\alpha})$ is a charge-preserving morphism:

$$\overline{P} \xrightarrow{\bar{\alpha}} \overline{Q} \xrightarrow{\bar{\beta}} \overline{R}$$

$$\downarrow^{\sigma} \qquad \downarrow^{\tau} \qquad v$$

$$\mathbb{Z}.$$

Definition 2.3: Let Fnc be the category whose objects are integral functions over finite, totally ordered posets, and whose morphisms are charge-preserving morphisms. We call Fnc the category of integral functions.

Remark 2.4: An important observation is that Fnc does not have arbitrary colimits. For example, the following two integral functions do not have a colimit. Let P = Q be totally-ordered posets on four elements; in particular, we write $P = Q = \{1 < 2 < 3 < 4\}$. Let $\sigma \colon \overline{P} \to \mathbb{Z}$ be the function

$$\sigma([i,j]) = \begin{cases} 1, & \text{if } i = 1, j = 3\\ 1, & \text{if } i = 2, j = 4\\ 0, & \text{otherwise,} \end{cases}$$

and let $\tau \colon \overline{Q} \to \mathbb{Z}$ be the function

$$\tau([i,j]) = \begin{cases} 1, & \text{if } i = 1, j = 4\\ 1, & \text{if } i = 2, j = 3\\ 0, & \text{otherwise.} \end{cases}$$

If a colimit existed, then it would come from gluing elements in P and gluing elements in Q until there is a common integral function. This leaves two contenders for the colimit:

- 1. The integral function $\mu: \overline{Z} \to \mathbb{Z}$ on the poset $Z = \{a < b < c\}$ that maps $[a,b] \mapsto 1$, $[a,c] \mapsto 1$, and everything else to zero. This is obtained by mapping 1 and 2 in both P and Q to a, 3 in P and Q to b, and 4 in P and Q to c.
- 2. The integral function $\nu : \overline{Z} \to \mathbb{Z}$ on the poset $Z = \{a < b < c\}$ that maps $[a, c] \mapsto 1$, $[b, c] \mapsto 1$, and everything else to zero. This is obtained by mapping 1 in both P and Q to a, 2 in P and Q to b, and 3 and 4 in P and Q to c.

We note that neither of these integral functions can be obtained from the other by gluing elements. This means that arbitrary colimits do not exist in Fnc.

Birth-Death Functor Fix a field k. The d-th birth-death functor ZB_d assigns to a filtration $F: P \to \Delta K$ the monotone integral function $\mathsf{ZB}_d(F): \overline{P} \to \mathbb{Z}$ defined as follows.

For every interval $[a,b] \in \overline{P}$, where $b \neq \top$, $\mathsf{ZB}_d[a,b]$ is the dimension of the k-vector space of d-cycles in the simplicial complex F(a) that are d-boundaries in the larger simplicial complex F(b). For an interval $[a,\top]$, $\mathsf{ZB}_d[a,\top]$ is simply the dimension of the vector space of d-cycles in F(a). The birth-death functor takes a filtration-preserving morphism (F,G,α) to the monotone-preserving morphism $(\mathsf{ZB}_i(F),\mathsf{ZB}_d(G),\bar{\alpha})$, which turns out to be a monotone-preserving morphism.

Möbius Inversion Functor Given a monotone integral function $f: \overline{P} \to \mathbb{Z}$, there is a unique integral function $\sigma: \overline{P} \to \mathbb{Z}$, called the Möbius inversion of f, such that for all $J \in P$,

$$f(J) = \sum_{I \in \overline{P}: I \le J} \sigma(I). \tag{2}$$

The functor MI assigns to every monotone-integral function its Möbius inversion. For every monotone-preserving morphism $(f, g, \bar{\alpha})$ in Mon, $(\text{MI } f, \text{MI } g, \bar{\alpha})$ is a charge-preserving morphism in Fnc.

Definition 2.5: We call the composition $\mathsf{PH}_* := \mathsf{MI} \circ \mathsf{ZB}_* : \mathsf{Fil}(K) \to \mathsf{Fnc}$ the **persistent homology functor**. It assigns to every filtration P in $\mathsf{Fil}(K)$ its persistence diagram $\mathsf{PH}_*(F)$ and to every filtration-preserving morphism (F, G, α) in $\mathsf{Fil}(K)$ the charge-preserving morphism $(\mathsf{PH}_*(F), \mathsf{PH}_*(G), \bar{\alpha})$.

An obvious but important observation is the following proposition, which follows immediately from the definition of the birth-death function and Equation (2).

Proposition 2.6: Let F be a filtration in Fil(K). Then, the total charge of its d-th persistence diagram, $\sum_{I \in \overline{P}} PH_d(F)(I)$, is the dimension of the d-th cycle space of K.

3 Combinatorial Transform for Geometric Complexes

Fix a geometric embedding $\phi: |K| \to \mathbb{R}^{N+1}$ of a simplicial complex K.

3.1 Constructing the Cellulation

Let $E := \{(v, v') : v, v' \in K^0\}$ be the set of all unordered, distinct pairs of vertices of K. For each pair of vertices $e = (v, v') \in E$, there is a unique plane in \mathbb{R}^{N+1} perpendicular to the vector $\phi(v) - \phi(v')$ through the origin; we denote that plane H_e . The intersection of H_e with the N-sphere, $S_e := H_e \cap \mathbb{S}^N$, is a great (N-1)-sphere of \mathbb{S}^n . By the Jordan-Brouwer separation theorem, $\mathbb{S}^N \setminus S_e$ has two connected components (often called *sides* or hemispheres) denoted arbitrarily by S_e^+ and S_e^- ; see [5, 15, 19]. Let $\mathcal{A} := \{S_e : e \in E\}$ be the multiset of all such great N-spheres. We call \mathcal{A} along with an assignment of a sign to each side of S_e , over all $e \in E$, a signed arrangement of spheres. The signed arrangement \mathcal{A} is essential if the following condition holds: $\bigcap_{e \in \mathcal{A}} S_e = \emptyset$.

The signed arrangement \mathcal{A} induces a cell complex on \mathbb{S}^N where every cell is described by whether it lies in S_e^- , S_e , or S_e^+ over every $S_e \in \mathcal{A}$. To define this cell complex, let $\{-,0,+\}^E$ denote the set of all functions from E to $\{-,0,+\}$. Consider the following partial order on $\{-,0,+\}$: 0 < - and 0 < +. This partial order extends to a partial order on the set of functions $\{-,0,+\}^E$, where $f \leq g$ if $f(e) \leq g(e)$, for all $e \in E$. Let $\Phi : \mathbb{S}^N \to \{-,0,+\}^E$ be the function that assigns to every direction $\mu \in \mathbb{S}^N$ the following vector indexed by elements $e \in E$:

$$\Phi(\mu)_e := \begin{cases}
- & \text{if } \mu \in S_e^- \\
0 & \text{if } \mu \in S_e \\
+ & \text{if } \mu \in S_e^+.
\end{cases}$$
(3)

Consider the subposet $\mathcal{P}(\mathcal{A}) := \{\Phi(\mu) : \mu \in \mathbb{S}^N\} \subseteq \{-,0,+\}^E$. The following proposition is a rewording of [4, Proposition 5.1.5].

Proposition 3.1: Let $\phi: |K| \to \mathbb{R}^{N+1}$ be geometric embedding and let \mathcal{A} be an induced signed arrangement of spheres on \mathbb{S}^N . If \mathcal{A} is essential, then the sets $\Phi^{-1}(f) \subseteq \mathbb{S}^N$, over all $f \in \mathcal{P}(\mathcal{A})$, are the cells of a cell complex $(\mathbb{S}^N, \mathcal{C})$. Furthermore, for every pair of such cells $C_1 := \Phi^{-1}(f)$ and $C_2 := \Phi^{-1}(g)$ in \mathcal{C} , $C_1 \leq C_2$ if and only if $f \leq g$ in $\mathcal{P}(\mathcal{A})$.

The signed arrangement \mathcal{A} associated to the piecewise linear embedding ϕ is essential if and only if $\bigcap_{e\in\mathcal{A}} S_e \neq \emptyset$ if and only if there is not a direction $\mu \in \mathbb{S}^n$ such that the height function ϕ_{μ} is constant on all of K. For example, if ϕ embedds K into a linear N-subspace of \mathbb{R}^{N+1} , then \mathcal{A} is not essential and we cannot apply Proposition 3.1. However, we can easily fix this problem by adding one more (N-1)-great sphere to the arrangement that is different from any of the (N-1)-great spheres already in \mathcal{A} . In general, for dim $(\bigcap_{e\in\mathcal{A}} S_e) = k$, we have to add k+1 great spheres to the arrangement \mathcal{A} .

3.2 Filtrations over Cellulation

Fix a geometric embedding $\phi: |K| \to \mathbb{R}^N$ and let $(\mathbb{S}^N, \mathcal{C})$ be the induced cellulation on the N-sphere as constructed above. Recall \mathcal{C} is a poset where $C_1 \leq C_2$ if C_1 is a face of C_2 . For every direction $\mu \in \mathbb{S}^n$, the height function ϕ_{μ} gives rise to an object of $\mathsf{Fil}(K)$. By construction of the cellulation, any two directions μ_1 and μ_2 give rise to the same object in $\mathsf{Fil}(K)$. Further, for every face relation $C_1 \leq C_2$, there is a natural filtration-preserving morphism from the filtration associated to C_2 to the filtration associated to C_1 . We now formalize this data as a functor $F: \mathcal{C} \to \mathsf{Fil}(K)$.

We start by defining F on the cells of C. Choose a cell $C \in C$ and a direction $\mu \in C$. Two vertices $v, v' \in K^0$ are related, denoted $v \sim_{\mu} v'$, if $\phi_{\mu}(v) = \phi_{\mu}(v')$. The relation \sim_{μ} is an equivalence relation. Note that $v \sim_{\mu} v'$ if and only if $\mu \in S_{(v,v')}$. Denote by P_{μ} the set of equivalence classes K^0/\sim_{μ} union the singleton $\{\top\}$. For two equivalence classes $[v]_{\mu}, [v']_{\mu}$ in P_{μ} , let $[v]_{\mu} \leq [v']_{\mu}$ if $\phi_{\mu}(v) \leq \phi_{\mu}(v')$. Make \top the top element. Thus P_{μ} is a finite, totally ordered lattice that is independent of the choice of $\mu \in C$. Note that $[v]_{\mu} \neq [v']_{\mu}$ if and only if $\mu \in S_{(v,v')}^+$ or $\mu \in S_{(v,v')}^-$. We now define the filtration $F(C) := F_{\mu} : P_{\mu} \to \text{Fil}$. For

every
$$[v]_{\mu}$$
, let

$$F_{\mu}([v]_{\mu}) := \{ \sigma \in K : \phi_{\mu}(\sigma) \le \phi_{\mu}(v) \}. \tag{4}$$

Let $F_{\mu}(\top)$ be the entire simplicial complex K. Note that $F_{\mu}([v]_{\mu})$ is a subcomplex of K and for $[v]_{\mu} \leq [v']_{\mu}$, $F_{\mu}([v]_{\mu})$ is a subcomplex of $F_{\mu}([v']_{\mu})$. In other words, F_{μ} is an object of Fil(K).

We now define F on the face relations $C_1 \leq C_2$ of C. Choose directions $v \in C_1$ and $\mu \in C_2$. There is a canonical bounded lattice function $\alpha: P_{\mu} \to P_{\nu}$ that turns out to be a filtration-preserving morphism $(F(C_2), F(C_1), \alpha)$ as follows. Since $\Phi(v) \leq \Phi(\mu)$, $[v]_{\mu} \subseteq [v]_{\nu}$ for every vertex $v \in K^0$. Let $\alpha([v]_{\mu}) := [v]_{\nu}$. Again, since $\Phi_{(v,v')}(\mu) \leq \Phi_{(v,v')}(v)$, we have that $[v]_{\mu} \leq [v']_{\mu}$ implies $[v]_{\nu} \leq [v']_{\nu}$. Let $\alpha(\top) := \top$. Thus α is a bounded lattice function. By piecewise linearity of ϕ , a simplex $\sigma \in F_{\mu}([v]_{\mu})$ if and only if $\phi_{\mu}(v_i) \leq \phi_{\mu}(v)$ for every vertex v_i of σ . Since α is order-preserving, $\phi_{\mu}(v_i) \leq \phi_{\mu}(v)$ implies $\phi_{\nu}(v_i) \leq \phi_{\nu}(v)$ and thus $\sigma \in F_{\nu}([v]_{\nu})$. Thus $(F_{\mu}, F_{\nu}, \alpha)$ is a filtration-preserving morphism. Now consider a third cell C_3 such that $C_1 \leq C_2 \leq C_3$ and choose a direction $w \in C_3$. Let $\beta: P_w \to P_{\mu}$ be the corresponding bounded lattice function. Then, the assignment $[v]_w \mapsto [v]_{\mu}$ is the composition $\alpha \circ \beta([v]_w)$. Thus the composition $F(C_1 \leq C_2) \circ F(C_2 \leq C_3)$ of filtration-preserving morphisms equals $F(C_1 \leq C_3)$.

3.3 Persistence Diagrams over Cellulation

Finally, we define the combinatorial PH transform associated to a geometric complex.

Definition 3.2: Let $\phi: |K| \to \mathbb{R}^{N+1}$ be a geometric complex, $(\mathbb{S}^N, \mathcal{C})$ the induced cellulation on the N-sphere, and $F: \mathcal{C} \to \mathsf{Fil}$ the functor as constructed above. The d-th combinatorial **PH transform** of ϕ is the functor $\mathsf{PH}_d \circ F: \mathcal{C} \to \mathsf{Fnc}$. The **combinatorial PH transform** of ϕ is the indexed set $\{\mathsf{PH}_d \circ F\}_{d \in \mathbb{N}}$, over all dimensions d.

Fix an embedding $\phi: |K| \to \mathbb{R}^{N+1}$ and let $\tilde{F}_d: \mathcal{C} \to \mathsf{Fnc}$ be its d-th combinatorial PH transform. The display locale [10, 11] of \tilde{F}_d , or generalized vineyard [7], has an interesting structure. By Proposition 2.6, there is a constant $n \in \mathbb{N}$ such that, for each cell $C \in \mathcal{C}$, the total charge of the persistence diagram $\tilde{F}_d(C)$ is n. Further, for every cell relation $C_1 \leq C_2$, the morphism $\tilde{F}(C_1 \leq C_2)$ taking the persistence diagram $\tilde{F}(C_2)$ to the persistence diagram $\tilde{F}(C_1)$ is charge-preserving. Thus, there is a unique charge associated to each connected component of the display locale.

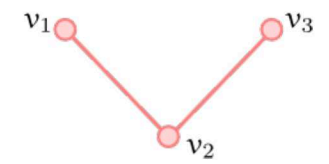


Figure 1: The V, embedded in \mathbb{R}^2 . This simplicial complex has three vertices and two edges. By exploring the combinatorial PH transform for this example, we illustrate each step of the construction.

4 Examples

In this section, we walk through two examples, one in \mathbb{R}^2 and one in \mathbb{R}^3 .

4.1 The V Example

We start with a simple example to step through the construction of the combinatorial PH transform of Definition 3.2. Specifically, our abstract simplicial complex consists of two edges connected along a single vertex: $K = \{\{v_1\}, \{v_2\}, \{v_3\}, \{v_1, v_2\}, \{v_2, v_3\}\}$. This complex is piecewise linearly embedded into \mathbb{R}^2 through the function $\phi \colon |K| \to \mathbb{R}^2$ with $\phi(v_1) = (-1, 1)$, $\phi(v_2) = (0, 0)$, and $\phi(v_3) = (1, 1)$. See Figure 1.

Cellulation The embedding ϕ induces a cellulation on the unit circle \mathbb{S}^1 of directions in \mathbb{R}^2 . We now walk through the construction of this cellulation. Let E be the set of unique pairs of vertices in K. In other words, let $E := \{(v_1, v_2), (v_1, v_3), (v_2, v_3)\}$. For every $(v_i, v_j) \in E$, let $H_{(i,j)}$ be the unique line through the origin that is perpendicular to the vector $\phi(v_i) - \phi(v_j)$. That is, $H_{(i,j)}$ is the line perpendicular to the line through the embeddings of v_i and v_j , as shown in Figure 2(a). The intersection $S_{(i,j)} := H_{(i,j)} \cap \mathbb{S}^1$ is a zero-sphere separating \mathbb{S}^1 into two components. As an arbitrary choice of signs, we denote the connected component containing (1,0) as $S_{(i,j)}^+$ and the other connected component as $S_{(i,j)}^-$. We now have a function $\Phi \colon \mathbb{S}^1 \to \{-,0,+\}^E$ as in Equation (3). Finally, let $(\mathbb{S}^1,\mathcal{C})$ be the cell complex as defined in Proposition 3.1; in particular, \mathcal{C} has six zero-cells and six one-cells. See Figure 2(b), where the 12 cells are labeled with their images under Φ . Notice that in this example, we have an essential arrangement. Since no two cells have the same label, we use C_X to denote the cell of \mathcal{C} labeled $X \in \{-,0,+\}^3$ (if such a cell exists). Again, by Proposition 3.1, we also have a partial order on the cells (e.g., $C_{(0++)} < C_{(+++)}$).

Objects of Filtration Functor The geometric embedding ϕ induces a functor $F: \mathcal{C} \to \text{Fil}$ of filtrations and filtration-preserving morphisms. We now walk through the construction of F on the four cells in the highlighted region of Figure 2(b).

Let μ be a direction in $C_{(+++)}$. Using the height function $\phi_{\mu} \colon |K| \to \mathbb{R}$, we obtain the following totally ordered lattice $[v_1]_{\mu} < [v_2]_{\mu} < [v_3]_{\mu}$; see Figure 3 (far left). To this, we add an additional equivalence class $[\top]_{\mu}$ as the top element of the lattice; in other words, we have

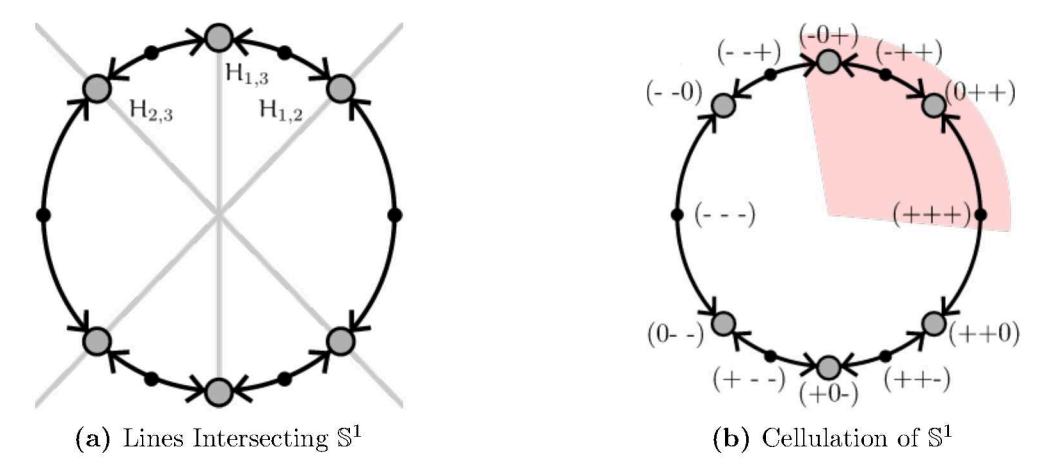


Figure 2: In (a), we see the three linear subpaces of \mathbb{R}^2 that are used to define the cellulation over \mathbb{S}^1 . In (b), each cell is labeled by a vector in $\{-,0,+\}^3$ according to which side of $S_{1,2}$, $S_{1,3}$, and $S_{2,3}$ the cell falls. For example, the vector (-++) labels the one-cell whose points are all in $S_{1,2}^-$, $S_{1,3}^+$, and $S_{2,3}^+$. The vector (0++) labels the zero-cell that is in $S_{1,2}$, $S_{1,3}^+$, and $S_{2,3}^+$. In fact, $C_{(0++)} = S_{1,2} \cap S_{1,3}^+ \cap S_{2,3}^+$. Note that no label is (000), and that all labels are distinct. The partial order of the cells is denoted by arrows (where $a \to b$ indicates that b < a).

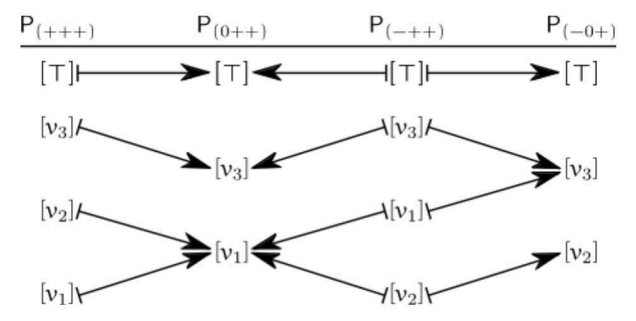


Figure 3: The bounded lattice functions for the three highlighted face relations in Figure 2(b). Notice that the two maps into $P_{(0++)}$ are nearly bijections, except for two vertices (v_1 and v_2) that map to the same equivalence class for both maps. This corresponds to the transposition of the two vertices between directions in $C_{(+++)}$ and $C_{(-++)}$. In fact, this property holds more generally for any face relation between codimension-one cells.

the totally ordered lattice:

$$[v_1]_{\mu} < [v_2]_{\mu} < [v_3]_{\mu} < [\top]_{\mu}.$$

Denote this lattice P_{μ} . Associated to P_{μ} is the filtration F_{μ} of Equation (4). Specifically,

$$\begin{split} F_{\mu}([v_{1}]_{\mu}) &:= \{v_{1}\} \\ F_{\mu}([v_{2}]_{\mu}) &:= \{v_{1}, v_{2}, \{v_{1}, v_{2}\}\} \\ F_{\mu}([v_{3}]_{\mu}) &:= \{v_{1}, v_{2}, v_{3}, \{v_{1}, v_{2}\}, \{v_{2}, v_{3}\}\} = K \\ F_{\mu}([\top]_{\mu}) &:= K. \end{split}$$

Notice that $F_{\mu}([v_1]_{\mu}) \subset F_{\mu}([v_1]_{\mu}) \subset F_{\mu}([v_1]_{\mu}) \subseteq F_{\mu}([\top]_{\mu})$. Moreover, this lattice and filtration are independent of the choice of μ . Therefore, we can define $[v_i]_{(+++)} := [v_i]_{\mu}$, $[\top]_{(+++)} := [\top]_{\mu}$, $P_{(+++)} := P_{\mu}$, and $P_{(+++)} := F_{\mu}$.

Next, consider the cell $C_{(-++)}$. We proceed as above and observe that $P_{(-++)}$ is the totally ordered lattice $[v_2]_{(-++)} < [v_1]_{(-++)} < [v_3]_{(-++)} < [\top]_{(-++)}$; see Figure 3 (middle right). For simplicity, we drop the subscripts of the equivalence classes when the cell (or direction) is clear from context and simply write $[v_2]$ from here on. Again, we use Equation (4) to define the filtration $F_{(-++)}$ is defined by

$$F_{(-++)}([v_2]) := \{v_2\}$$

$$F_{(-++)}([v_1]) := \{v_1, v_2, \{v_1, v_2\}\}$$

$$F_{(-++)}([v_3]) := \{v_1, v_2, v_3, \{v_1, v_2\}, \{v_2, v_3\}\} = K$$

$$F_{(-++)}([\top]) := K.$$

We note the partial order on $P_{(-++)}$ given by the heights of vertices in direction μ induces the following partial order on the simplicial complexes: $F_{(-++)}([v_2]) \subset F_{(-++)}([v_1]) \subset F_{(-++)}([v_3]) \subseteq F_{(-++)}([\top])$.

The zero-cells of C are exactly the directions that two vertices are seen at the same height. For example, in $C_{(0++)}$, the heights of v_1 and v_2 are the same (since $\phi_{\mu}(v_1) = \phi_{\mu}(v_2)$), and this height is less than $\phi_{\mu}(v_3)$. Thus, the lattice $P_{(0++)}$ is the following total order on the induced equivalence classes: $[v_1] < [v_3] < [\top]$. In addition, the filtration $F_{(0++)}$ is defined by

$$F_{(0++)}([v_1]) := \{v_1, v_2, \{v_1, v_2\}\}$$

$$F_{(0++)}([v_3]) := \{v_1, v_2, v_3, \{v_1, v_2\}, \{v_2, v_3\}\} = K$$

$$F_{(0++)}([\top]) := K.$$

Again, we notice the inclusion of subcomplexes: $F_{(0++)}([v_1]) \subset F_{(0++)}([v_3]) \subseteq F_{(0++)}([\top])$. Finally, $P_{(-0+)}$ is the lattice $[v_2] < [v_3] < [\top]$, with corresponding filtration $F_{(-0+)}$ defined by $F_{(-0+)}([v_2]) = \{v_2\}$ and $F_{(-0+)}([v_3]) = \{v_1, v_2, v_3, \{v_1, v_2\}, \{v_2, v_3\}\} = K = F_{(-0+)}([\top])$. See Figure 3.

Arrows of the Filtration Functor We now walk through the construction of F on the three arrows in the highlighted region of Figure 2(b). Consider the face relation $C_{(0++)} \leq$

 $C_{(+++)}$. We define the filtration-preserving morphism $(F(C_{(+++)}), F(C_{(0++)}, \alpha))$ as follows. For each vertex v_i , we have the inclusion $[v_i]_{(+++)} \subseteq [v_i]_{(0++)}$. Indeed,

$$[v_1]_{(+++)} = \{v_1\} \subseteq \{v_1, v_2\} = [v_1]_{(0++)}$$

$$[v_2]_{(+++)} = \{v_2\} \subseteq \{v_1, v_2\} = [v_2]_{(0++)}$$

$$[v_3]_{(+++)} = \{v_3\} \subseteq \{v_3\} = [v_3]_{(0++)}$$

$$[\top]_{(+++)} = \emptyset \subseteq \emptyset = [\top]_{(0++)}$$

As a consequence, $F([v]_{(+++)}) \subset F([v]_{(0++)})$ for all objects $[v] \in P_{(+++)}$. Thus, we can define $\alpha(F([v]_{(+++)})) := F([v]_{(0++)})$. In other words, we have collapsed two equivalence classes in the lattice and consequently the filtration, and left the rest untouched. See Figure 3.

Combinatorial PH Transform Now that we have a filtration functor, we can apply the persistent homology pipeline of [21] and described in Section 2.2. Our next step is to apply the birth-death functor ZB: Fil \rightarrow Mon. To keep the notation as simple as possible, we use the field $\mathsf{k} = \mathbb{Z}/2\mathbb{Z}$. We explain this functor by looking at how it behaves on the objects $F_{(+++)}$ and $F_{(0++)}$, and the arrow $F_{(+++)} \rightarrow F_{(0++)}$. Recall from above that $P_{(+++)}$ is the totally ordered lattice $[v_1] < [v_2] < [v_3] < [\top]$. For simplicity of notation, we use [i,j] to represent $[[v_i], [v_j]]$. Thus, $P_{(+++)}$ is the nine element poset shown on the left hand side of Figure 4(a). Similarly, $P_{(0++)}$ is the poset shown on the right hand side of Figure 4(a). The bounded lattice function $\alpha : P_{(+++)} \rightarrow P_{(0++)}$ (the leftmost map in Figure 3) induces a bounded lattice function $\bar{\alpha} : P_{(+++)} \rightarrow P_{(0++)}$. In particular,

$$[1,1]_{(0++)} = \bar{\alpha}([1,1]_{(+++)}) = \bar{\alpha}([1,2]_{(+++)}) = \bar{\alpha}([2,2]_{(+++)}),$$

$$[1,3]_{(0++)} = \bar{\alpha}([1,3]_{(+++)}) = \bar{\alpha}([2,3]_{(+++)}),$$

$$[1,\top]_{(0++)} = \bar{\alpha}([1,\top]_{(+++)}) = \bar{\alpha}([2,\top]_{(+++)}),$$

$$[3,3]_{(0++)} = \bar{\alpha}([3,3]_{(+++)}),$$

$$[3,\top]_{(0++)} = \bar{\alpha}([3,\top]_{(+++)}), \text{ and}$$

$$[\top,\top]_{(0++)} = \bar{\alpha}([\top,\top]_{(+++)}).$$

These three equivalences are illustrated with pink shading in Figure 4(a). If $i \neq 1$, then K has no i-cycles and hence ZB_i is trivial everywhere. The values of ZB_0 on the objects in $\overline{P_{(+++)}}$ and $\overline{P_{0++}}$ are illustrated in Figure 4(b), with the induced monotone-preserving morphism.

Finally, we apply the Möbius Inversion Functor MI: Mon \to Fnc. Again, we illustrate this functor by describing how it behaves on $\mathsf{ZB}_0(\overline{P_{(+++)}} \to \overline{P_{(0++)}})$. First, we define $\mathsf{MI}_{(+++)} := \mathsf{MI}(\mathsf{ZB}_0(\overline{P_{(+++)}})$ to be the unique function $\sigma \colon \overline{P_{(+++)}} \to \mathbb{Z}$ that satisfies Equation (2), where $f = \mathsf{ZB}_0(\overline{P_{(+++)}})$. In particular, for $x \in \overline{P_{(+++)}}$

$$\mathsf{MI}_{(+++)}(x) = \begin{cases} 1 & x \in \{[2,2], [3,3], [1,\top]\} \\ 0 & \text{otherwise.} \end{cases}$$

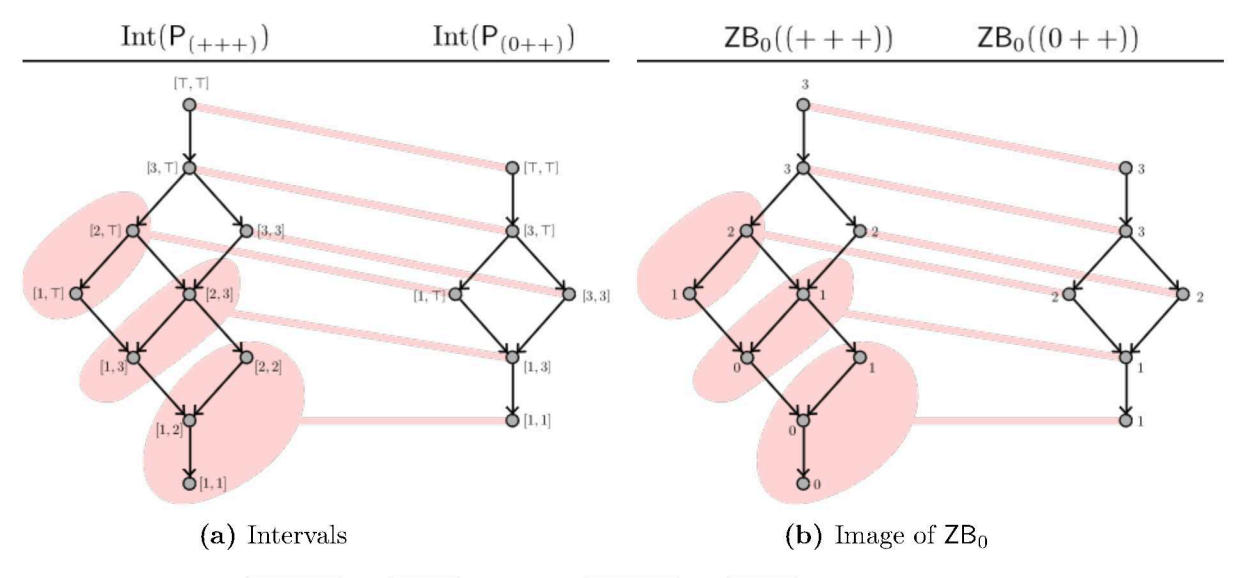


Figure 4: The maps $\overline{P_{(+++)}} \to \overline{P_{0++}}$ and $\mathsf{ZB}_0(\overline{P_{(+++)}} \to \overline{P_{0++}})$. In both maps, the objects in the same pink region get mapped to the same object in the codomain. Using the field $\mathsf{k} = \mathbb{Z}/2\mathbb{Z}$, for $b \neq \top$, $\mathsf{ZB}_0[a,b]$ counts the number of zero-cycles in the simplicial complex F(a) that are zero-boundaries in the larger simplicial complex F(b). $\mathsf{ZB}_0[a,\top]$ is a count of the number of vertices in F(a).

In other words, the augmented persistence diagram (defined in [13, Def. 1]) has three points: (2,2), (3,3), and $(1,\infty)$. This corresponds to the persistence diagram with one off-diagonal point, namely $(1,\infty)$, which corresponds to the connected component born at the height of v_1 . Next, we consider the cell $S_{(0++)}$. Let $x \in \overline{P_{(0++)}}$. Then,

$$\mathsf{MI}_{(0++)}(x) = \begin{cases} 1 & x \in \{[1,1],[3,3],[1,\top]\} \\ 0 & \text{otherwise.} \end{cases}$$

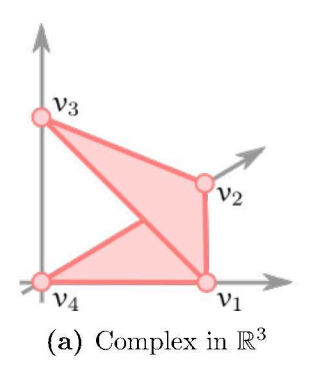
Moreover, the map $\mathsf{MI}_{(+++)} \to \mathsf{MI}_{(0++)}$ corresponds to mapping the points in the following way: $[2,2]_{(+++)} \mapsto [1,1]_{(0++)} = [2,2]_{(0++)}$, $[3,3]_{(+++)} \mapsto [3,3]_{(0++)}$, and $[1,T]_{(+++)} \mapsto [1,T]_{(0++)}$. We note that while [2,2] and [1,T] have distinct birth heights in $\mathsf{MI}_{(+++)}$, their images [1,1] and [1,T] have the same birth height in $\mathsf{MI}_{(0++)}$.

4.2 3D Example

We now consider a geometric complex embedded in \mathbb{R}^3 . Specifically, let K be the following abstract simplicial complex known as a book with two pages (see Figure 5(a)):

$$K = \{\{v_1\}, \{v_2\}, \{v_3\}, \{v_1, v_2\}, \{v_2, v_3\}, \{v_1, v_3\}, \{v_1, v_2, v_3\}, \{v_1, v_4\}, \{v_2, v_4\}, \{v_1, v_2, v_4\}\}.$$

This complex is piecewise linearly embedded into \mathbb{R}^3 through the function $\phi: |K| \to \mathbb{R}^2$ with $\phi(v_1) = (1,0,0)$, $\phi(v_2) = (0,1,0)$, $\phi(v_3) = (0,0,1)$ and $\phi(v_0) = (0,0,0)$. Note that the affine space spanned by the points $\{v_1, v_2, v_3, v_4\}$ is \mathbb{R}^3 , indicating that the vertices of K are





(b) Cellulation of \mathbb{S}^2

Figure 5: A geometric complex in \mathbb{R}^3 with the induced cellulation of \mathbb{S}^2 . The cellulation depends only on the vetices of the complex. Since the vertices are in general position, each great circle on \mathbb{S}^2 is distinct.

in general position. Rather than go through the whole pipeline again, we investigate the cell complex and the poset of equivalence classes of vertices associated to each cell.

Let $(\mathbb{S}^2, \mathcal{C})$ be the cell complex defined in Proposition 3.1. This cellulation has 24 twocells, one for each permutation of the vertices. (Note that if we were to add one more vertex to K that there would then be more permutations of the vertices than cells of the cellulation due to geometric constraints). Each of the 36 one-cells correspond to where two vertices are at the same height and the remaining two vertices are at distinct heights. There are two types of zero-cells: (type-1) eight have degree six and correspond to exactly three vertices at the same height, and (type-2) six have degree four and correspond to two vertices at one height and the other two vertices at another height. See Figure 5(b).

For each vector $X \in \{-,0,+\}^6$, we use $C_{(X)}$ to denote the cell of \mathcal{C} labeled X according to which side of $S_{1,2}$, $S_{1,3}$, $S_{2,3}$, $S_{1,4}$, $S_{2,4}$, and $S_{3,4}$ the cell falls (if such a cell exists). For example, $C_{(+---++)} = S_{1,2}^+ \cap S_{1,3}^- \cap S_{2,3}^- \cap S_{1,4}^- \cap S_{2,4}^+ \cap S_{3,4}^+$. The faces of $C_{(+---++)}$ are:

$$\{C_{(+---+)}, C_{(0---+)}, C_{(+0--+)}, C_{(+---+0)}, C_{(+0-0+0)}, C_{(0---+0)}, C_{(000-++)}\}.$$

In fact, every two-cell in this cellulation has seven faces (itself, three one-cells, and three zero-cells). In other words, every two-cell is a topological triangle. Some labelings of zero-cells do not exist. For example, no cell is labeled (00 - - + +). By contradiction, suppose there exists $\mu \in C_{(00--++)}$. Then, since the first coordinate is zero, $\mu \in S_{1,2}$, which implies that $[v_1]_{\mu} = [v_2]_{\mu}$. In addition, since the second coordinate is zero, $\mu \in S_{2,3}$, which implies that $[v_2]_{\mu} = [v_3]_{\mu}$. Thus, $[v_1]_{\mu} = [v_2]_{\mu}$, which means that $\mu \in S_{2,3}$, a contradiction.

To see what happens at a type-1 zero-cell, consider $P_{(000-++)}$. In particular, the equivalence classes for the vertices induced by a direction vector in $C_{(000-++)}$ is:

$$[v_1]_{(000-++)} = [v_2]_{(000-++)} = [v_3]_{(000-++)}$$

 $[v_4]_{(000-++)}$
 $[\top].$

In general, all type-1 zero-cells have three vertices sharing an equivalence class. To see

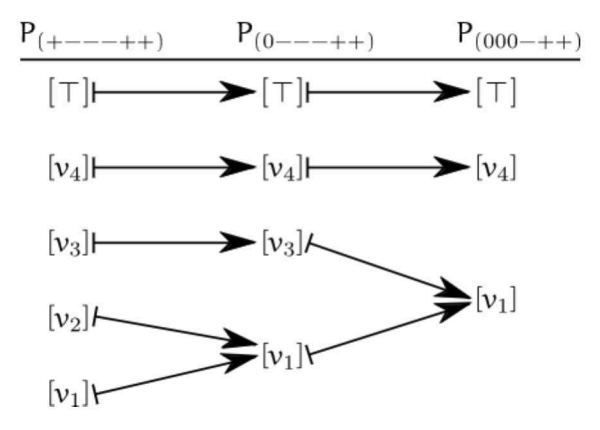


Figure 6: Face relations induce surjective poset maps. These maps, in turn, induce arrows in Fil.

what happens at a type-2 zero-cell, consider $P_{(0--+0)}$. Here, we have the following equivalence classess:

$$[v_1]_{(0---+0)} = [v_2]_{(0---+0)}$$
$$[v_3]_{(0---+0)} = [v_4]_{(0---+0)}$$
$$[\top].$$

In general, all type-2 zero-cells partition the vertices into two equivalence classes, each of size two (and one additional equivalence class for \top).

For geometric complexes in \mathbb{R}^3 or higher, we can look at compositions of proper face relations. Consider the following two face relations: $C_{(000-++)} < C_{(0---++)} < C_{(+---+)}$. These face relations induced posets of equivalence classes of the vertices, as well as the maps connecting these posets, are given in Figure 6. These two maps corresponds to the equivalences classes $[v_1]_{(+---++)} \neq [v_2]_{(+---++)}$ being mapped to the same equivalence class $[v_1]_{(0---++)}$ in $P_{(0---++)}$, followed by the equivalences classes $[v_1]_{(0---++)} \neq [v_3]_{(0---++)}$ equivalence classes in $P_{(+---++)}$ being mapped to the same equivalence class $[v_1]_{(000-++)}$ in $P_{(000-++)}$. Observe that the map $P_{(+---++)} \rightarrow P_{(000-++)}$ is exactly this composition resulting in collapsing three equivalence classes in $P_{(+---++)}$ (namely, $[v_1]$, $[v_2]$, and $[v_3]$) to one equivalence class.

5 Discussion

By taking a combinatorial approach to persistent homology, we are able to express the PH transform of a geometric complex as a functor from the cellulation of a sphere to the category of combinatorial persistence diagrams. This point of view may be applied to any application that involves a parameterized family of persistence diagrams. For example, consider time-varying data [6, 7, 18, 23]. Assuming the data is finite, there is a cellulation of the real line (time parameter) such that any two times on the same cell have the same combinatorial persistence diagram. The resulting family of combinatorial persistence diagrams connected

by charge-preserving morohisms provides a categorical framework in which to talk about all the persistence diagrams at once in a cohesive manner.

We hope this paper will start conversations on parameterized families of combinatorial persistence diagrams in general and not just for the PH transform. There are many questions to ask. For example, consider a cell complex (X, \mathcal{C}) on any space X and a functor $F: \mathcal{C} \to \mathsf{Fnc}$. What are its global co-sections? Does the edit distance of McClearly and Patel lead to a stability result for such functors? These are just a few questions worth asking.

Acknowledgements The first author acknowledges Vin de Silva for a late night conversation about counting cells and David L. Millman for generating Figure 5(b).

References

- [1] Pankaj K. Agarwal, Herbert Edelsbrunner, John Harer, and Yusu Wang. Extreme elevation on a 2-manifold. *Discrete & Computational Geometry*, 36(4):553–572, 2006.
- [2] Robin Lynne Belton, Brittany Terese Fasy, Rostik Mertz, Samuel Micka, David L. Millman, Daniel Salinas, Anna Schenfisch, Jordan Schupbach, and Lucia Williams. Reconstructing embedded graphs from persistence diagrams. *Computational Geometry: Theory and Applications*, 2020.
- [3] Leo M. Betthauser. *Topological Reconstruction of Grayscale Images*. PhD thesis, University of Florida, 2018.
- [4] A. Björner, M. Las Vergnas, B. Strumfels, N. White, and G. Ziegler. *Oriented Matroids*. Cambridge University Press, 1993.
- [5] Luitzen E. J. Brouwer. L.E.J. Brouwer Collected Works, volume 2: Geometry, Analysis, Topology and Mechanics. North-Holland/American Elsevier, North Holland, Amsterdam, 1976. Chapter 6. New Methods in Topology. Proof from 1911.
- [6] Peter Bubenik and Michael J. Catanzaro. Multiparameter persistent homology via generalized Morse theory. arXiv 2107.08856, 2021.
- [7] David Cohen-Steiner, Herbert Edelsbrunner, and Dmitriy Morozov. Vines and vineyards by updating persistence in linear time. In *Proceedings of the Twenty-Second Annual Symposium on Computational Geometry*, pages 119–126, New York, NY, USA, 2006. ACM.
- [8] Lorin Crawford, Anthea Monod, Andrew X Chen, Sayan Mukherjee, and Raúl Rabadán. Predicting clinical outcomes in glioblastoma: An application of topological and functional data analysis. *Journal of the American Statistical Association*, pages 1–12, 2019.

- [9] Justin Curry, Sayan Mukherjee, and Katharine Turner. How many directions determine a shape and other sufficiency results for two topological transforms. arXiv:1805.09782, 2018.
- [10] Justin Michael Curry. Sheaves, Cosheaves, and Applications. PhD thesis, The University of Pennsylvania, 2014. Also available at arxiv:1303.3255.
- [11] Vin De Silva, Elizabeth Munch, and Amit Patel. Categorified Reeb graphs. Discrete & Computational Geometry, 55(4):854–906, 2016.
- [12] Brittany Terese Fasy, Samuel Micka, David L. Millman, Anna Schenfisch, and Lucia Williams. Challenges in reconstructing shapes from Euler characteristic curves. In *Proceedings of the Fall Workshop on Computational Geometry*, 2018. Also available at arXiv:1811.11337.
- [13] Brittany Terese Fasy, Samuel Micka, David L. Millman, Anna Schenfisch, and Lucia Williams. A faithful representation of the PHT and other topological transforms. arXiv:1912.12759, 2020.
- [14] Robert Ghrist, Rachel Levanger, and Huy Mai. Persistent homology and Euler integral transforms. *Journal of Applied and Computational Topology*, 2(1-2):55–60, 2018.
- [15] Allen Hatcher. Algebraic Topology. Cambridge University Press, Cambridge, 2000.
- [16] Christoph Hofer, Roland Kwitt, Marc Niethammer, Yvonne Höller, Eugen Trinka, and Andreas Uhl. Constructing shape spaces from a topological perspective. In *International Conference on Information Processing in Medical Imaging*, pages 106–118. Springer, 2017.
- [17] Qitong Jiang, Sebastian Kurtek, and Tom Needham. The weighted Euler curve transform for shape and image analysis. In *Proceedings of the IEEE/CVF Conference on Computer Vision and Pattern Recognition Workshops*, pages 844–845, 2020.
- [18] Woojin Kim and Facundo Mémoli. Spatiotemporal persistent homology for dynamic metric spaces. Discrete & Computational Geometry, 66(3):831–875, 2021.
- [19] Henri Lebesgue. Sur l'invariance du nombre de dimensions d'un espace et sur le théorème de M. Jordan relatif aux variétés fermées. Comptes Rendus de l'Académie des Sciences Series I Mathematics, 1911.
- [20] Clément Maria, Steve Oudot, and Elchanan Solomon. Intrinsic topological transforms via the distance kernel embedding. In Sergio Cabello and Danny Z. Chen, editors, Proceedings of the Thirty-Sixth Annual International Symposium on Computational Geometry, volume 164 of Leibniz International Proceedings in Informatics (LIPIcs), pages 56:1–56:15, Dagstuhl, Germany, 2020. Schloss Dagstuhl–Leibniz-Zentrum für Informatik.

- [21] Alexander McCleary and Amit Patel. Edit distance and persistence diagrams over lattices. SIAM Journal on Applied Algebra and Geometry, 6(2):134–155, 2022.
- [22] Samuel Adam Micka. Searching and Reconstruction: Algorithms with Topological Descriptors. PhD thesis, Montana State University, 2020.
- [23] Elizabeth Munch, Katharine Turner, Paul Bendich, Sayan Mukherjee, Jonathan Mattingly, and John Harer. Probabilistic Fréchet means for time varying persistence diagrams. *Electronic Journal of Statistics*, 9(1):1173 1204, 2015.
- [24] Emily Riehl. Category Theory in Context. Dover Publications, 2013.
- [25] Katharine Turner, Sayan Mukherjee, and Doug M. Boyer. Persistent homology transform for modeling shapes and surfaces. *Information and Inference: A Journal of the IMA*, 3(4):310–344, 2014.

A Notation and Definitions

Posets Given a finite, totally ordered poset P, denote by $\bot \in P$ its smallest element and by $\top \in P$ the largest element. A function $\alpha : P \to Q$ between two finite, totally ordered posets is a bounded monotone function if $f(\top) = \top$, $f(\bot) = \bot$, and for all $a \le b$, $\alpha(a) \le \alpha(b)$.

For a finite, totally ordered poset P, let $\overline{P} := \{[a,b] \subseteq P : a \leq b\}$ be its set of non-empty intervals with the following partial relation: $[a,b] \preceq [c,d]$ if $a \leq c$ and $b \leq d$. Its bottom element is $[\bot,\bot]$ and its top element is $[\top,\top]$. A bounded monotone function $\alpha:P\to Q$ between two finite, totally ordered posets induces a bounded monotone function $\bar{\alpha}:\bar{P}\to\bar{Q}$ where $\bar{\alpha}([a,b]):=[\alpha(a),\alpha(b)]$; see [21] for a proof.

Categories and Functors In this paper, we assume that the reader is familiar with categories and functors. We defer to [24] for an introduction to category theory. In Table 1, we provide notations used in this paper.

Table 1: Notations for categories and functors. We assume C is a category and $a, b, c \in \mathsf{ob} \mathsf{C}$.

ob C	objects in C
$\operatorname{Hom}_{C}(a,b)$	the set of morphisms or arrows between a and b in C
0	composition of morphisms
1_a	the identity morphism in $\operatorname{Hom}_{C}(a,a)$